Nanoscale

Accepted Manuscript

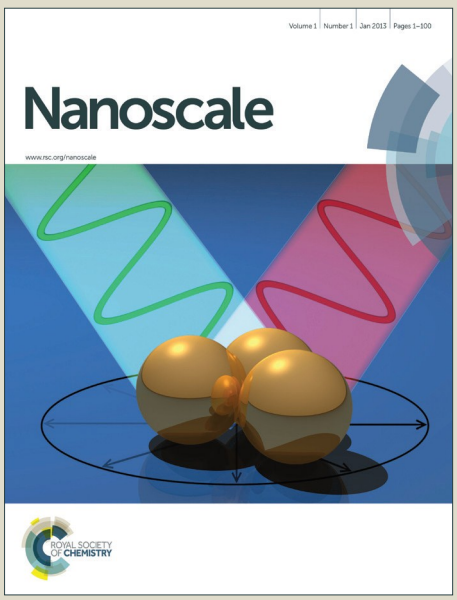

This is an *Accepted Manuscript*, which has been through the Royal Society of Chemistry peer review process and has been accepted for publication.

Accepted Manuscripts are published online shortly after acceptance, before technical editing, formatting and proof reading. Using this free service, authors can make their results available to the community, in citable form, before we publish the edited article. We will replace this *Accepted Manuscript* with the edited and formatted *Advance Article* as soon as it is available.

You can find more information about *Accepted Manuscripts* in the Information for Authors.

Please note that technical editing may introduce minor changes to the text and/or graphics, which may alter content. The journal's standard Terms & Conditions and the Ethical guidelines still apply. In no event shall the Royal Society of Chemistry be held responsible for any errors or omissions in this *Accepted Manuscript* or any consequences arising from the use of any information it contains.

ROYAL SOCIETY OF CHEMISTRY

www.rsc.org/nanoscale

Journal Name

RSCPublishing

ARTICLE

The Controllable Poly-crystalline Bilayer and Multilayer Graphene Film Growth by Reciprocal Chemical Vapor Deposition

Cite this: DOI: 10.1039/xoxxoooooox

Received ooth January 2012,
Accepted ooth January 2012

DOI: 10.1039/xoxxoooooox

www.rsc.org/

Qinke Wu[1], Seong Jun Jung[1], Sungkyu Jang[1], Joohyun Lee[1], Insu Jeon[2], Hwansoo Suh[2], Yong Ho Kim[1,3], Young Hee Lee[4]*, Sungjoo Lee[1,5,6]* and Young Jae Song[1,4,7]*

We report a selective growth of large-area bilayer graphene film and multilayer graphene film on copper. This growth was achieved by introducing a reciprocal chemical vapor deposition (CVD) process that took advantage of an intermediate h-BN layer as a sacrificial template for graphene growth. A thin h-BN film, initially grown on the copper substrate using CVD methods, was locally etched away during the subsequent graphene growth under residual H_2 and CH_4 gas flows. Etching of the h-BN layer formed a channel that permitted the growth of additional graphene adlayers below the existing graphene layer. Bilayer graphene typically covers an entire Cu foil with domain sizes of 10–50 μm, whereas multilayer graphene can be epitaxially grown to form islands a few hundreds of microns in size. This new mechanism, in which graphene growth proceeded simultaneously with h-BN etching, suggests a potential approach to control graphene layers for engineering the band structures of large-area graphene for electronic device applications.

Introduction

A major breakthrough toward realizing industrial applications of graphene has been made using chemical vapor deposition (CVD) methods.[1] Graphene films 30 inches in width can be produced using a roll-to-roll process in a CVD system.[2] Monolayer graphene grown on a platinum surface using CVD methods can yield a carrier mobility up to 7100 cm^2/V s, comparable to the mobilities obtained from exfoliated graphene mounted on SiO_2/Si.[3] Recently, another type of CVD graphene was grown directly on h-BN/Cu substrates, followed by a study of the catalytic growth mechanism.[4,5] The application of monolayer graphene to electronic devices remains limited, however, by graphene's unique zero band gap dispersion relation.[6] Luckily, the band gap of AB-stacked bilayer graphene may be tuned under an electric field or using chemical conjugation.[7,8] Systematic growth and study of bilayer graphene films, however, has not been enough, although a variety of CVD studies have been applied to high-quality monolayer graphene with large domain sizes and few or no grain boundaries.[9–12] Here, we report a unique method for the selective growth of a multilayer graphene and poly-crystalline bilayer graphene (pBLG) film with a typical domain size of ~50 μm. This growth was achieved by introducing a reciprocal CVD process that took advantage of an intermediate CVD h-BN film as a sacrificial template for graphene growth. This new method suggests a high potential for graphene with controllable number of layers for graphene-based science and device applications.

Experimental

Chemical polishing of Cu

A Cu foil from Alfa Aesar (no. 13382) was used as the growth substrate and was cut into pieces 3 x 5 cm in size. The Cu foil was then chemically polished in a solution containing 20 g potassium persulfate, 98%, and 500 mL DI water under an applied current of 0.6 A for 10 min to remove impurities and the native oxide. The Cu foil was then rinsed with HF (20%) three times to remove the etchant residue. Finally, the foil was dried under N_2 gas.

Growth of the h-BN and graphene layers

A large area h-BN film, which acted as a sacrificial template during multilayer/bilayer graphene growth, was grown on the Cu foils (prepared as described above) using LP-CVD methods (with a pressure of 7 mTorr), as reported previously.[4,13] A borazine source was introduced into the chamber along with the N_2 carrier gas at 1050 ℃. The thickness of the h-BN layer could be controlled according to the h-BN growth time: h-BN films of monolayer, 2 nm or 5 nm thick were grown over 25 min, 40 min or 60 min, respectively, as shown in the Figure S2. And the thickness and surface uniformity were confirmed by AFM in Figure S3 and S4. After the h-BN film had been deposited, graphene was CVD-grown under 5 sccm H_2 and 0.5 sccm CH_4

Nanoscale Accepted Manuscript

for 12 hours at 1050 ℃. Figure S1(a) illustrates the layer growth process in detail, and Figure S1(b) lists the different conditions used during the graphene growth step to produce graphene/h-BN heterostructure growth and epitaxial multilayer graphene growth.

Transfer of graphene

Each graphene layer was transferred from the Cu foil to other substrates (SiO_2/Si, quartz, or a Si_3N_4 TEM grid) by spin-coating a 950PMMA A6 (Microchem) supporting scaffold onto the graphene surface with a spin speed of 45000 rpm for 55 seconds. The sample was then cured by heating on a hot plate at 90 ℃ for 5 minutes. The underlying Cu was etched away using an iron (III) chloride solution (with a concentration of 0.1 g mL^{-1}) over 12 hours. The PMMA/graphene film was rinsed twice in deionized water and once in HCl (0.3 g mL^{-1}) for 10 minutes to remove residual iron (III) chloride. The film was then rinsed again in deionized water. Finally, the sample was transferred onto the target substrate. After the sample had been transferred and dried, the PMMA was removed by heating in acetone (on a hot plate at 52 ℃) for three minutes.

Characterization

X-ray photoelectron spectroscopy (XPS) studies were carried out on an ESCA Lab2201-XL spectrometer using an Al Kα X-ray excitation source. The structure and crystallinity were characterized using a transmission electron microscope (TEM 2100F, JEOL) equipped with a selected-area electron diffraction (SAED) instrument. Raman spectroscopy was performed using a laser micro-Raman spectrometer (Kaiser Optical System Model RXN1, 532 nm excitation wavelength).

Results and discussion

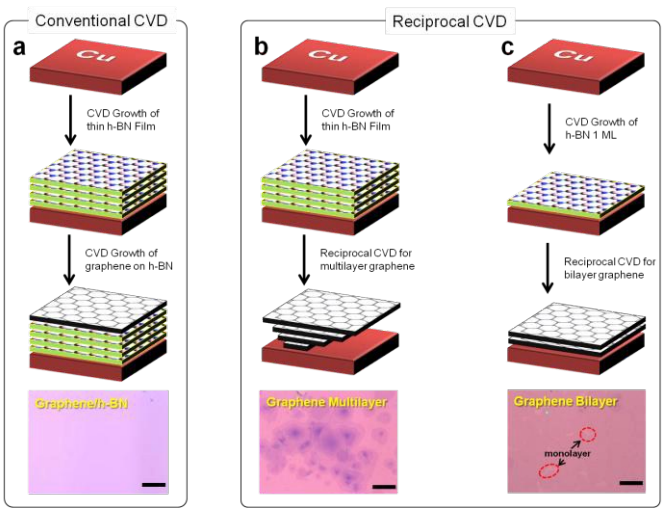

Figure 1. Schematic diagram illustrating the CVD processes involved in graphene growth, along with the corresponding OM images. (a) shows the growth of a graphene/h-BN heterostructure using a conventional CVD process.[4] (b)–(c) describe the growth of epitaxial multilayer graphene or poly-crystalline bilayer graphene using a reciprocal CVD process. The scale bars in all OM images indicate 50 μm.

When combined with the *in situ* CVD growth of a graphene/h-BN film, an intermediate empty gap could be formed by etching the initial h-BN layers to enable the controlled CVD growth of additional graphene layers as shown in **Figure 1**. A thin h-BN film, initially grown on the copper substrate by CVD, provided a sacrificial template that will be slowly etched away during the subsequent graphene growth by residual hydrogen atoms present in the H_2 gas flow or produced by the decomposition of the carbon precursors (CH_4). The carbon precursors then diffused into the gap to form a graphene adlayer beneath the first graphene layer (the top-most layer). Once the Cu surface becomes fully covered with the first graphene layer, the graphene adlayers ceased their growth beneath the first graphene layer, as shown in Figure 1(b)-(c). The parameters that governed graphene/h-BN growth (Figure 1(a)) and multilayer graphene growth (Figure 1(b)) are discussed in the supporting information (Figure S1).

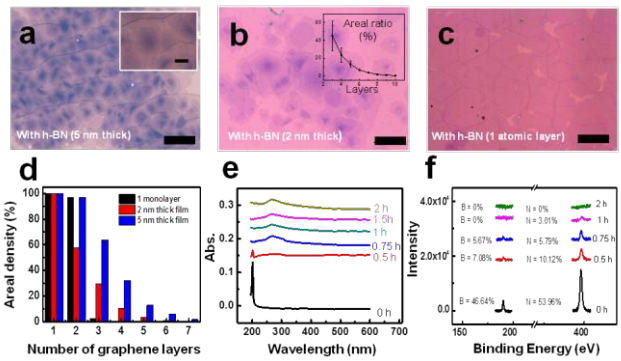

Figure 2. The thickness of the h-BN layer in the reciprocal CVD process determined the properties of the resulting graphene layer. (a)–(c) OM images of graphene grown using h-BN films 5 nm, 2 nm, or 1 monolayer thick, respectively. The inset of (a) shows a magnified view of the film, and the inset of (b) shows the areal ratio of each layer compared with the area of the mother (2nd) layer. (d) shows a histogram of the areal density versus the number of graphene layers present in the samples shown in (a)–(c). (e)–(f) The UV-visible absorption spectra and XPS data measured at different growth times confirmed that the h-BN layer had been etched away, and no traces of B or N remained. The scale bars indicate 50 μm in (a)–(c) and 10 μm in the inset of (a).

Optical microscopy (OM) images shown in Figure 1(b) revealed that the multilayer graphene islands were formed with tens of microns in size. Careful observations revealed that the edge angles of the different graphene layers within a given graphene island (intra-island angles) were perfectly (100%) parallel between the 3rd layer and the higher-index layers. Only the edge angles (>93%) between the 2nd and 3rd layers were not universally parallel (see Figure S6 in the supporting information). As the fully covered top graphene layer (mother layer) was shared by all of the multilayer graphene islands, the edge angles of the adjacent graphene islands (inter-island angle) were mainly 0 ° and 60 °, with a small distribution of angles near 30 ° and 85 ° (see Figure S7 in the supporting information). Finally, the process was further optimized using one atomic monolayer of CVD h-BN to synthesize a bilayer graphene film, as shown in Figure 1(c). The h-BN etching process played a critical role in forming bilayer or multilayer graphene. Three

Nanoscale Accepted Manuscript

This journal is © The Royal Society of Chemistry 2012

different thicknesses of the h-BN layer (5 nm, 2 nm, or 1 atomic layer, which are grown by controlling the growth time as shown in Figure S2) were used as a template. Figures 2(a)–(c) show OM images of graphene grown on each h-BN layer, revealing very different size and thickness distributions of graphene islands. The graphene layer grown using a 5 nm thick h-BN film yielded the largest number of layers, although the island areas were small. Graphene grown on a 2 nm thick h-BN layer, however, yielded fewer layers with a larger average area. The inset in Figure 2(b) shows the growth speed of each layer formed using a 2 nm thick h-BN film. The first graphene layer covered the entire surface and was shared among all graphene islands; therefore, the areal ratio of the third layer up to the tenth layer was compared with the area of the mother 2nd layer. The use of a one atomic monolayer thick h-BN as a template mainly yielded bilayer graphene (>96.7% in Figure 2(c)). Figure 2(d) shows a histogram summarizing the areal density (coverage) of each number of graphene layers shown in Figures 2(a)–(c). When a h-BN monolayer was used as a sacrificial film, therefore, the gap thickness between a Cu surface and the first graphene layer is about ~0.35 nm. This gap thickness is not enough to grow many layers of graphene, so Figure 2(d) indicates that the bilayer graphene covers > 96.7 % of the surface. The key for this is, we think, the larger domain size of h-BN monolayer, which reduces the number of nucleation seeds. The less number of nucleation seeds for h-BN as well as (in-situ) sequential and slow CVD process for grapheme can grow a polycrystalline bilayer graphene film having very large coverage. To compare, we also grow graphene on bare copper substrate with the same growth conditions and find it out that in this case we can only get monolayer graphene, as shown in Figure S5. The number of CVD graphene layers could be controlled by using an h-BN film with a well-defined thickness as a sacrificial spacer and growth template. Even bilayer graphene films could be intentionally grown.

The complete etching of the initial h-BN layer with only graphene was confirmed using UV-visible absorption spectroscopy and XPS measurements for the samples with different growth time of reciprocal CVD. Figure 2(e) shows the UV-visible absorption spectroscopy data obtained after 0, 0.5, 0.75, 1.0, 1.5, or 2.0 hours of graphene growth. The spectrum collected from the initial sample without graphene (black color) revealed a very high and sharp h-BN peak at 201 nm, indicating the presence of the high quality h-BN film.[14] As the graphene

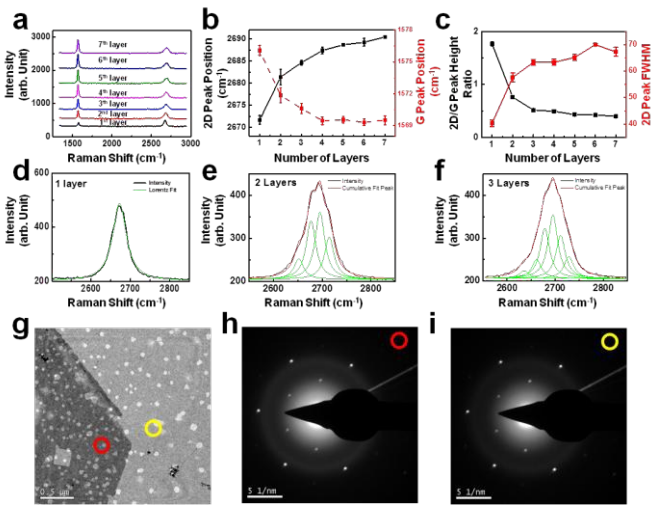

Figure 3. Quality and epitaxial growth of multilayer graphene. (a) Raman spectra obtained from each layer in the multilayer graphene, from the monolayer to the seventh layer. (b) The positions of the 2D band (black) and G band (red) shifted as the number of graphene layers present increased. (c) Full-width half-maximum values of the 2D band and the 2D/G ratio. (d)–(f) 2D band peak fits obtained from monolayer, bilayer, or trilayer graphene. (g) TEM image near the boundary between the two layers. (h)–(i) SAED data obtained from the red (h) or yellow (i) circles in (g).

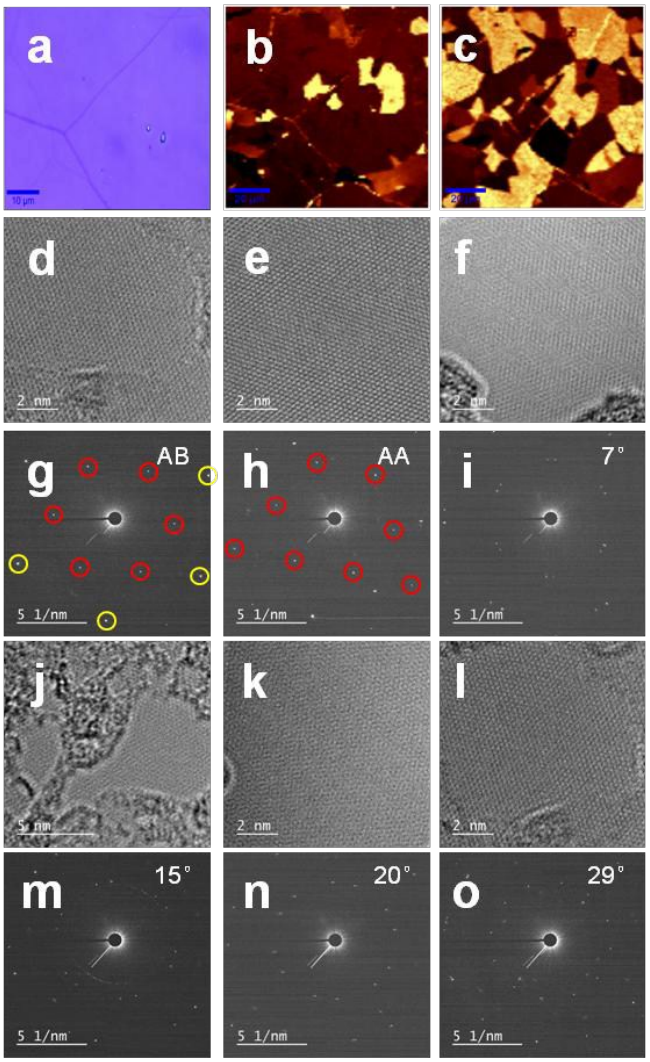

Figure 4. The domains and epitaxial growth of large-area bilayer graphene. (a) OM image obtained from large-area bilayer graphene. (b)–(c) Two-dimensional Raman mapping of the G band and 2D band over the sample area shown in (a). (d)–(f) and (j)–(l) Atomic-resolution TEM images measured over an AB stacked bilayer, AA stacked bilayer, and twisted bilayer characterized by twisted angles of 7°, 15°, 20° and 29°. (g)–(i) and (m)–(o) show the SAED data obtained from the samples presented in (d)–(f) and (j)–(l). The scale bars indicate 10 μm in (a) and 20 μm in (b)–(c).

Nanoscale Accepted Manuscript

growth time increased, the h-BN peak got smaller and broader and finally disappeared completely after one hour of graphene growth. The graphene peak at 265 nm appeared after 0.5 hours and continued to grow with time.[4] The etching of the h-BN layer was further verified using XPS techniques by measuring the B and N elemental compositions of the same samples (Figure 2(f)). The peaks corresponding to B and N disappeared completely after 2 hours of graphene growth. All the studies presented in Figures 2(e)–(f) were performed using the multilayer graphene shown in Figure 2(b) (2 nm thick h-BN). The model for graphene growth by a reciprocal CVD process is illustrated in Figure S9, and in Figure S10 shows the details about bilayer and multilayer growth cases.

The multilayer graphene films were carefully examined for quality using confocal Raman spectroscopy and transmission electron microscopy (TEM). A graphene island with more than seven layers thick was intentionally selected. Figure 3(a) shows a series of Raman spectra corresponding to high-quality graphene. The intensity height, peak position, and G-to-2D peak ratio in the Raman spectrum depended on the number and stacking of the graphene layers.[15] The epitaxy of the multilayer graphene was characterized by measuring the 2D and G peak positions, the 2D/G peak height ratio, and the full width at half maximum (FWHM) of the 2D peak. The 2D peak position was located at 2671.7 cm^{-1} for the monolayer graphene, and a blue shift was observed upon the addition of more layers (black curve in Figure 3(b)). The G peak position displayed a red shift from 1576.1 cm^{-1} (monolayer), and quickly reached a maximum of 1569.5 cm^{-1} at the fourth layer (red curve in Figure 3(b)). Figure 3(c) shows a high 2D/G peak ratio of 1.77 and a sharp 2D peak with a FWHM of 40.26 cm^{-1} for monolayer graphene. As the number of graphene layers increased, the 2D/G peak height ratio decreased to 0.76 for the bilayer and reached a maximum at the fourth layer. The 2D peak width increased rapidly and reached a maximum at the fourth layer. Figure 3(d)–(f) show Lorentzian curve fits of the 2D peaks corresponding to monolayer, bilayer, or trilayer graphene, respectively, with the fit parameters obtained from each sample. The Raman spectral features also agreed well with previous studies of epitaxial graphene flakes that were mechanically exfoliated from HOPG.[11,15,16] Epitaxial growth on the atomic scale was confirmed using TEM measurements and selected area electron diffraction (SAED) measurements. Figure 3(g) shows a well-defined angle of 120 ° at one corner of the higher-index layer. Figures 3(h)–(i) show the SAED data obtained from two different layers (red and yellow circles). These data were consistent with the crystallinity corresponding to AB stacking.[17] Multilayer graphene was confirmed to have grown epitaxially by a reciprocal CVD process involving simultaneous graphene growth and h-BN etching.

Figure 4(a) is an OM image of a bilayer graphene film and Figures 4(b)–(c) show a two-dimensional Raman mapping of the G band and 2D band. Although >96.7% of the entire sample area was covered with bilayer graphene, the G band and 2D band mapping revealed sharp domain boundaries with allowing only a few discrete contrasts. The intensity of the Raman G band could be strongly enhanced at the twisted angle (at 12.5 °) of the bilayer graphene, when laser excitation energy of 2.33 eV is used, due to a singularity in the joint density of states of the twisted bilayer graphene (tBLG).[19] The area, width, and position of the 2D band as well as the 2D/G ratio also depended on the twisted angle. The results suggested that the entire bilayer graphene film was not pure bilayer graphene of an AB stacking structure, but rather poly-crystalline with a few selected twisted angles with very sharp boundaries. The domains of a poly-crystalline bilayer graphene (pBLG) film are characterized by the twisted angle between layers, and not by the structural boundary of the top layer only. A typical domain size in a bilayer graphene film (as defined by twisted angles)

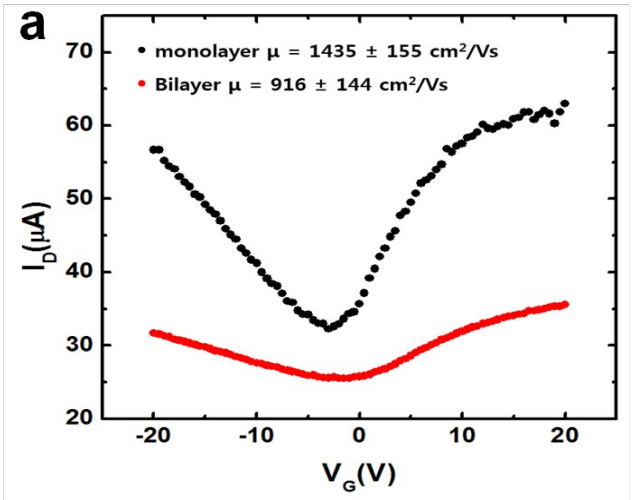

Figure 5. (a) The Electrical transfer characteristics (drain current I_d vs. gate voltage V_G) of monolayer and bilayer graphene.

can be smaller than the corresponding value in monolayer graphene (defined by the structural boundaries). In our work, the maximum domain size of the poly-crystalline bilayer graphene was found to be ~50 μm.

High-resolution TEM and SAED measurements were collected from the poly-crystalline bilayer graphene. Figures 4(d)–(f) and 4(j)–(l) show atomic-resolution TEM images, and Figures 4(g)–(i) and 4(m)–(o) present the corresponding electron diffraction data. Figure 4(g) reveals variations in the peak intensities, as indicated by the yellow and red circles, suggesting that Figure 4(d) corresponded to a bilayer having an AB stacking structure. The diffraction pattern and intensities shown in Figure 4(h) indicated that Figure 4(e) corresponded to AA stacking. Figures 4(f), (j), (k), and (l) present the dimensions of the Moiré patterns produced by the twisted angles of the poly-crystalline bilayer graphene. Twisted angles of 7 °, 15 °, 20 °, and 29 ° were measured from the corresponding SAED data. These twisted angles in a poly-crystalline bilayer graphene match well with commensurate rotations between two graphene layers.[18,19] In a few cases, twisted trilayers were observed (see Figure S12 in the supporting information). Additionally, more than 30 field effect transistor (FET) devices were prepared using poly-

Nanoscale Accepted Manuscript

This journal is © The Royal Society of Chemistry 2012

crystalline bilayer graphene films with channel sizes of 20 μm x 10 μm. These device measurements were consistent with the characteristics of bilayer graphene (see Figure 5). The further optimization of h-BN layer quality on Cu substrates, therefore, can be applied to improve the domain sizes and the twisted orientations of the bilayer graphene on the large scale.

Conclusions

In conclusion, poly-crystalline bilayer graphene and multilayer graphene were grown on Cu substrates using a reciprocal CVD process in which graphene was grown while an h-BN layer was simultaneously etched away. During graphene growth on the h-BN/Cu substrate under optimized conditions, residual hydrogen atoms present in the H_2 gas flow or produced by the decomposition of CH_4 etched away the h-BN film to enable the growth of an additional graphene layer. UV-visible absorption spectroscopy and XPS measurements confirmed that the h-BN buffer layer was etched away completely. The domain sizes and structures of the epitaxial multilayers and poly-crystalline bilayers of graphene were studied using confocal Raman spectroscopy and TEM/SAED methods. The reciprocal CVD process involving simultaneous graphene growth and h-BN etching constitutes a significant advancement for controlling the number of CVD graphene layers for graphene-based science and device applications.

Acknowledgements

This research was supported by the Institute for Basic Science (IBS) and Basic Science Research Program through the National Research Foundation of Korea (NRF) funded by the Korean government (MSIP) (Grant Numbers: IBS-R011-D1, 2011-0030046, 2012R1A1A1041416, NRF-2014M3C1A3001208, 2009-0083540, 2012R1A1A2020089 and 2013M3A6B1078873).

Notes and references

[1]SKKU Advanced Institute of Nanotechnology (SAINT), Sungkyunkwan University (SKKU), Suwon 440-746, Korea.

[2]Nano Electronics Lab., Samsung Advanced Institute of Technology, Suwon 443-803, Korea.

[3]Department of Chemistry, Sungkyunkwan University (SKKU), Suwon 440-746, Korea.

[4]Center for Integrated Nanostructure Physics, Institute for Basic Science (IBS), Sungkyunkwan University, Suwon 440-746. Korea.

[5]Center for Human Interface Nanotechnology (HINT), Sungkyunkwan University (SKKU), Suwon 440-746, Korea.

[6]College of Information and Communication, Sungkyunkwan University (SKKU), Suwon 440-746, Korea.

[7]Department of Physics, Sungkyunkwan University (SKKU), Suwon 440-746, Korea.

* Corresponding authors: yjsong@skku.edu (YJS); leesj@skku.edu (SL); leeyoung@skku.edu (YHL), Sungkyunkwan University (SKKU), Suwon 440-746, Korea.

Electronic Supplementary Information (ESI) available: The growth conditions, statistical studies of OM images and high-resolution STM/TEM measurements for multi-/bi- layer graphene are discussed in detail.

1 X. Li, W. Cai, J. An, S. Kim, J. Nah, D. Yang, R. Piner, A. Velamakanni, I. Jung, E. Tutuc, S. K. Banerjee, L. Colombo and R. S. Ruoff, *Science*, 2009, **324**, 1312–1314.
2 S. Bae, H. Kim, Y. Lee, X. Xu, J.-S. Park, Y. Zheng, J. Balakrishnan, T. Lei, H. R. Kim, Y. I. Song, Y.-J. Kim, K. S. Kim, B. Özyilmaz, J.-H. Ahn, B. H. Hong and S. Iijima, *Nat. Nanotechnol.*, 2010, **5**, 574–578.
3 L. Gao, W. Ren, H. Xu, L. Jin, Z. Wang, T. Ma, L.-P. Ma, Z. Zhang, Q. Fu, L.-M. Peng, X. Bao and H.-M. Cheng, *Nat. Commun.*, 2012, **3**, 699.
4 M. Wang, S. K. Jang, W.-J. Jang, M. Kim, S.-Y. Park, S.-W. Kim, S.-J. Kahng, J.-Y. Choi, R. S. Ruoff, Y. J. Song and S. Lee, *Adv. Mater.*, 2013, **25**, 2746–2752.
5 M. Wang, M. Kim, D. Odkhuu, N. Park, J. Lee, W.-J. Jang, S.-J. Kahng, R. S. Ruoff, Y. J. Song and S. Lee, *ACS Nano*, 2014, **8**, 5478–5483.
6 K. S. Novoselov, *Science*, 2004, **306**, 666–669.
7 D. L. Duong, S. M. Lee, S. H. Chae, Q. H. Ta, S. Y. Lee, G. H. Han, J. J. Bae and Y. H. Lee, *Phys. Rev. B*, 2012, **85**, 205413.
8 Y. Zhang, T.-T. Tang, C. Girit, Z. Hao, M. C. Martin, A. Zettl, M. F. Crommie, Y. R. Shen and F. Wang, *Nature*, 2009, **459**, 820–823.
9 H. Zhou, W. J. Yu, L. Liu, R. Cheng, Y. Chen, X. Huang, Y. Liu, Y. Wang, Y. Huang and X. Duan, *Nat. Commun.*, 2013, **4**.
10 J.-H. Lee, E. K. Lee, W.-J. Joo, Y. Jang, B.-S. Kim, J. Y. Lim, S.-H. Choi, S. J. Ahn, J. R. Ahn, M.-H. Park, C.-W. Yang, B. L. Choi, S.-W. Hwang and D. Whang, *Science*, 2014, **344**, 286–289.
11 S. Lee, K. Lee and Z. Zhong, *Nano Lett.*, 2010, **10**, 4702–4707.
12 Y. Hao, M. S. Bharathi, L. Wang, Y. Liu, H. Chen, S. Nie, X. Wang, H. Chou, C. Tan, B. Fallahazad, H. Ramanarayan, C. W. Magnuson, E. Tutuc, B. I. Yakobson, K. F. McCarty, Y.-W. Zhang, P. Kim, J. Hone, L. Colombo and R. S. Ruoff, *Science*, 2013, **342**, 720–723.
13 K. H. Lee, H.-J. Shin, J. Lee, I. Lee, G.-H. Kim, J.-Y. Choi and S.-W. Kim, *Nano Lett.*, 2012, **12**, 714–718.
14 R. Y. Tay, M. H. Griep, G. Mallick, S. H. Tsang, R. S. Singh, T. Tumlin, E. H. T. Teo and S. P. Karna, *Nano Lett.*, 2014, **14**, 839–846.
15 A. Gupta, G. Chen, P. Joshi, S. Tadigadapa and Eklund, *Nano Lett.*, 2006, **6**, 2667–2673.
16 D. Graf, F. Molitor, K. Ensslin, C. Stampfer, A. Jungen, C. Hierold and L. Wirtz, *Nano Lett.*, 2007, **7**, 238–242.
17 K. Yan, H. Peng, Y. Zhou, H. Li and Z. Liu, *Nano Lett.*, 2011, **11**, 1106–1110.
18 R. W. Havener, H. Zhuang, L. Brown, R. G. Hennig and J. Park, *Nano Lett.*, 2012, **12**, 3162–3167.
19 T. G. Mendes-de-Sa, A. M. B. Goncalves, M. J. S. Matos, P. M. Coelho, R. Magalhaes-Paniago and R. G. Lacerda, *Nanotechnology*, 2012, **23**, 475602.
20 J. M. B. Lopes dos Santos, N. M. R. Peres and A. H. Castro Neto, *Phys. Rev. Lett.*, 2007, **99**.

Nanoscale Accepted Manuscript